Characterization of Pt Nanoparticles Encapsulated in Al_2O_3 and Their Catalytic Efficiency in Propene Hydrogenation†

Jung Whan Yoo, David Hathcock, and Mostafa A. El-Sayed*

Laser Dynamics Laboratory, School of Chemistry and Biochemistry, Georgia Institute of Technology, Atlanta, Georgia 30332-0400

Received: June 5, 2001; In Final Form: July 9, 2001

Pt nanoparticles supported in nanoporous Al_2O_3 catalyst are prepared by reduction of K_2PtCl_4 solution using H_2 in the presence of Al_2O_3 and poly(acrylic acid) as capping material. After thorough washing with water to remove Pt nanoparticles located on the external surface of the Al_2O_3 and drying at 70 °C for 12 h, they were used in propene hydrogenation to evaluate catalytic activity as measured by the value of the activation energy in the temperature range between 30 and 90 °C. The Pt nanoparticles are characterized by using transmission electron microscopy (TEM). The particles in Pt/Al_2O_3 are found to be encapsulated and uniformly dispersed inside the Al_2O_3; however, the size and shapes are not clearly seen. After extraction of the Pt nanoparticles from the Al_2O_3 channels by using an ethanol-diluted HF solution, various shapes such as truncated octahedral, cubic, tetrahedral, and spherical with a size around 5 nm are observed. The encapsulated particles have various shapes but are smaller in size than those prepared in K_2PtCl_4 solution with polyacrylate in the absence of Al_2O_3. Using FT-IR studies, the capping material initially used in Pt/Al_2O_3 is not found in the Al_2O_3 channels. This might be due to the fact that the polymer (average MW 2100) is too large to be accommodated within the Al_2O_3 pores. The nanopores of Al_2O_3 have several roles in the synthesis of these nanoparticles. It allows for uniform dispersion and encapsulation of Pt nanoparticles. It controls the Pt sizes with narrow distribution that is determined by the pore dimension (5.8 nm). It protects against metal particle aggregation and produces various shapes even in the absence of the capping material. Using these Pt nanoparticles, the catalysis of hydrogenation of propene gas was studied. The initial rates, reaction order, rate constants, and activation energy for the hydrogenation are determined by use of mass spectrometric techniques. The activation energy is found to be 5.7 kcal/mol, which is about one-half that previously reported for catalysis by Pt metal deposited in SiO_2 and TiO_2 synthesized by using H_2PtCl_6 and $Pt(allyl)_2$ by impregnation method.

Introduction

Metal nanoparticles are of considerable interest because they can exhibit physical and chemical properties, due to quantum size effects, that differ from those of bulk metals. They possess unique electronic, optical, and catalytic properties that are different from bulk macrocrystallites.[1−4] These nanoparticles are presently under intensive study for applications in optoelectronic devices,[5] ultrasensitive chemical and biological sensors,[6−8] and as catalysts in chemical and photochemical reactions.[9,10] In particular, they have a characteristic high surface-to-volume ratio, and consequently large fractions of the metal atoms are on the surface and thus are accessible to reactant molecules and available for catalysis.[11] They have been used as catalysts[12,13] in hydrogenation, hydroformylation, hydration, and various other reactions.

Heterogeneous catalysts, in particular, porous materials such as alumina, silica, and zeolite, have many advantages as supports because of their high surface areas, shape/size selectivity, and easy separation from the reaction mixtures. For these reasons, the use of Pt nanoparticles deposited on such porous materials has been increased recently.[14−17] These catalysts have typically been prepared by impregnation/ion-exchange methods by immersing the calcined porous materials in an aqueous solution of various Pt precursors such as H_2PtCl_6,[14] $Pt(NH_3)_4(NO_3)_2$,[15] $Pt(AcAc)_2$,[15] $Pt(NH_3)_4Cl_2$,[16] $Pt(NH_3)_4(OH)_2$,[16] and $Pt(allyl)_2$.[17] The dried Pt catalysts are calcined in flowing air and reduced in flowing H_2 around 450 °C. These methods are very complex, take a long time, and give mainly amorphous (no shaped) nanoparticles. These Pt nanoparticles have been used in the catalysis of unsaturated hydrocarbon hydrogenation and aromatization to understand the dependence of the catalytic properties on the particle size.[18]

Another method to make metal nanoparticles has used capping materials, polyacrylate and poly(*N*-vinyl-2-pyrrolidone) (PVP), in the precursor solution.[19,20] The capping material has roles not only to prevent particle aggregation but also to control shape and size.[19] Relatively speaking, the latter method is simple and can obtain good shaped nanoparticles.

The hydrogenation of various hydrocarbon compounds has been employed from time to time as a convenient probe reaction for evaluating the catalytic properties of supported Pt metals. Platinum is a superior catalyst for a variety of hydrocarbon conversion reactions.[21] Under suitable reaction conditions (reactant composition, pressure, and reaction temperature), platinum is active for hydrogenation reaction. Propene hydrogenation has also been used for this purpose.[17,22]

In the present study, Pt nanoparticles deposited in nanoporous Al_2O_3 are synthesized using K_2PtCl_4 solution and poly(acrylic acid) as the capping material in the presence of Al_2O_3. Their

† Part of the special issue "Noboru Mataga Festschrift".

* Author to whom correspondence should be addressed. Tel.: 404-894-0292. Fax: 404-894-0294. E-mail: mostafa.el-sayed@chemistry.gatech.edu.

10.1021/jp0121318 CCC: $22.00
Published on Web 10/04/2001

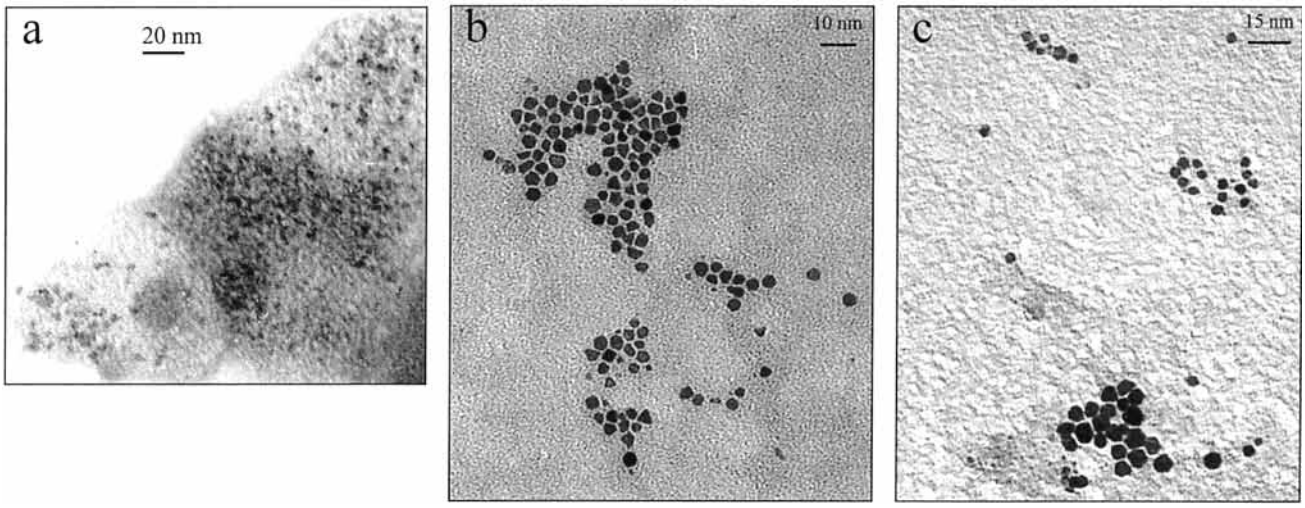

Figure 1. TEM images of (a) Pt nanoparticles synthesized in the presence of Al_2O_3 and polyacrylate with a concentration ratio of 1:5 Pt to polyacrylate, (b) Pt nanoparticles extracted from (a) using 20 wt % HF solution, and (c) Pt particles extracted from sample, prepared by impregnation the (a) sample with Pt particles solution synthesized with 1:5 concentration ratio of K_2PtCl_4 to polyacrylate.

particles size/shapes through extraction technique using acid solution and the capping material are clearly characterized by transmission electron microscopy (TEM) and FT-IR. The catalytic activity, as measured by the value of the activation energy, is studied for the heterogeneous hydrogenation of propene and compared with other literature values synthesized by different methods and on different support material. The observed difference is discussed.

Experimental Section

Chemicals. K_2PtCl_4 (99.99%), sodium polyacrylate (average MW 2100), and Al_2O_3 (neutral, surface area 155 m^2/g, pore size 5.8 nm) were obtained from Aldrich. All solutions were prepared using doubly deionized water. Propene (99.9995%) and hydrogen (99.995%) purchased from Matheson Company were used without further purification. The purity of the propene was checked by mass spectrometry.

Catalyst Preparation. Preparation method of the Pt/Al_2O_3 catalyst is similar to that used by Rampino and Nord[23] and Henglein et al.[24] except for the addition of Al_2O_3. A 5 g sample of Al_2O_3 was added to 250 mL of solution made by adding 1 mL of 0.1 M sodium polyacrylate (capping material) to 249 mL of 8.0×10^{-5} M K_2PtCl_4. The initial concentration ratio of K_2PtCl_4 to polyacrylate was 1:5. The pH of the solution was then adjusted to 7 with 0.1 M HCl and purged with Ar for 20 min. Pt complexes were reduced by bubbling H_2 for 5 min. The solution was left for 12 h in the dark. Subsequently, it was filtered, washed with 5 L of water, and dried at 70 °C for 12 h.

For comparison, Pt/Al_2O_3 catalyst without addition of the poly(acrylic acid) was prepared under the same condition as that used in the presence of the polymer.

TEM and FT-IR Measurements. TEM was used to determine the particle size/shapes of Pt nanoparticles supported in Al_2O_3. For making a TEM sample of supported Pt on Al_2O_3 catalyst dried and washed after separation from the Pt/Al_2O_3 solution, it was suspended in ethanol (99.9 wt %) by ultrasonification for 1 h after grinding the Pt/Al_2O_3 and subsequently left in the Pt/Al_2O_3 solution for several hours. The suspended sample was deposited on a carbon grid by slow evaporation at room temperature. To clearly image the particles encapsulated in Al_2O_3, the particles must be extracted from the Al_2O_3 channels. A small amount of Pt/Al_2O_3 synthesized was added to a 20 wt % HF solution diluted with ethanol. The Al_2O_3 was gradually dissolved after stirring this solution. The Pt nanoparticles in 20 wt % HF solution were separated and washed with ethanol several times via centrifuge. TEM images were taken by using a JEM 100C operated at an acceleration voltage of 100 kV at a magnification of 100000−190000 at room temperature. The particle size/shapes were determined from the enlarged TEM images.

FT-IR spectra are recorded on pellets made of the sample with a Bruker IFS 66/S FT-IR spectrometer. Typically, 100 scans were accumulated for each spectrum with resolution 2 cm^{-1} by OPUS 2.0 software. FT-IR spectra were recorded in the range of 2300−1000 cm^{-1}. Pressure was applied to the powder sample until the pellet made a clear disk.

Results and Discussion

A. Particle Characterization. Figure 1a shows a TEM image of the Pt/Al_2O_3 prepared from a 1:5 concentration ratio of K_2PtCl_4 to polyacrylate. In this figure, the Pt nanoparticles are shown as small black dots that are homogeneously dispersed within the Al_2O_3 support. The Pt nanoparticles appear to be located within the Al_2O_3 channels (Al_2O_3 pore size is 5.8 nm) since the diameter of the Pt nanoparticles observed is less than 5 nm. No Pt particles are observed on the external surfaces. As indirect evidence, the diameter of Pt nanoparticles in solution prepared under the same conditions is about 8 nm,[25] which is larger in size than that of the Pt/Al_2O_3 pore aperture. Actually, the Pt/Al_2O_3 solution in the presence of polymer after H_2 reduction for 12 h is colorless, which is quite different from those of Pt nanoparticles synthesized in solution in the absence of Al_2O_3 or SiO_2, otherwise, under the same synthetic conditions. The solution of the particles prepared in solution with no alumina or with silica gives a bright golden color. These observations can be explained as follows. Pt salt dissolved in water diffuses into the Al_2O_3 channel and strongly interacts and adsorbs on Al_2O_3 channel walls.[26] Reduced Pt atoms begin nucleation and growth uniformly within the Al_2O_3 channel. In the case of Pt/SiO_2, however, though Pt precursor diffuses into the SiO_2 channels (pore size is 6 nm), there might not be any interaction between the precursor and the support and the growth takes place in solution with the polymer capping. Therefore, the color of the resultant solution is bright golden, which is the same as the solution of Pt nanoparticles with the capped polymer.

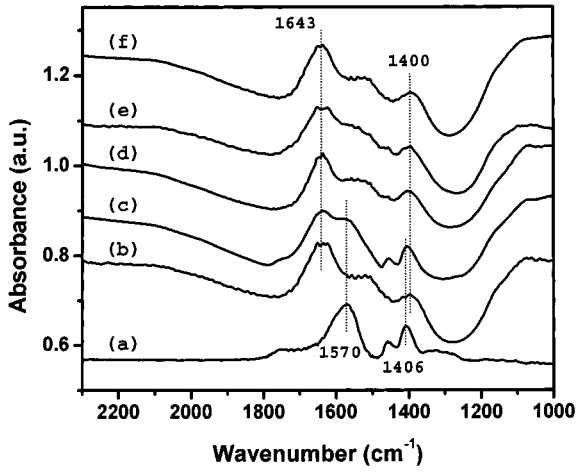

Figure 2. FT-IR spectra of (a) polyacrylate, (b) alumina, (c) mixture of polyacrylate and alumina, (d) as-synthesized Pt/Al_2O_3 with polyacrylate, (e) thermal-treated (d) at 155 °C, and (f) as-synthesized Pt/Al_2O_3 prepared without polyacrylate.

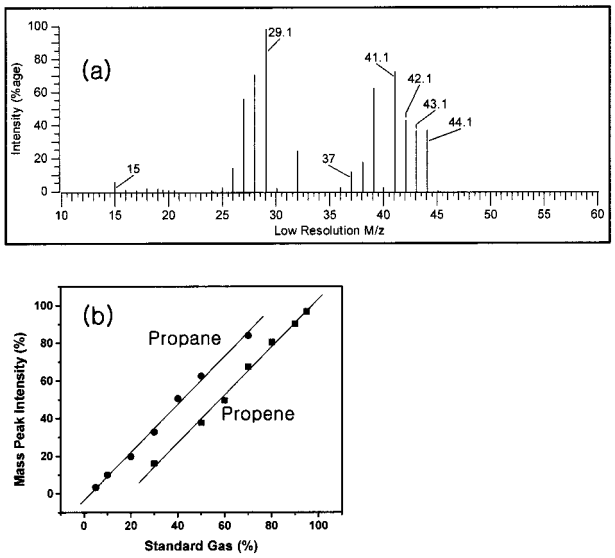

Figure 3. Mass spectrum of propene hydrogenation over Pt/Al_2O_3 catalyst (a) and calibration curve between propene and propane (b).

Encapsulated Pt particles were extracted from Al_2O_3 channels by dissolving the support with an HF solution. Figure 1b shows clear Pt size and shapes, indicating various shapes such as truncated octahedral, tetrahedral, cubic, and spherical with considerable narrow distribution of 4−5 nm size. The variety in shapes is quite different from that observed for samples prepared in solution with only capping polymer under the same conditions. In such a case, more than 90% of truncated octahedral Pt nanoparticles were normally observed.[25] This difference in particle shape distribution can likely be attributed to the influence of the Al_2O_3 channel used for the growth of Pt particles with different shapes.

To compare size/shapes of Pt nanoparticles formed by the encapsulation method and those prepared in solution, the Pt encapsulated in Al_2O_3 was impregnated with Pt nanoparticles solution which was prepared from a 1:5 concentration ratio of K_2PtCl_4 to polyacrylate. The TEM images of the Pt particles extracted from the sample are shown in Figure 1c. First of all, a large difference in the size is clearly shown. Larger particles formed in the solution are in the range of 8−10 nm and are primarily truncated octahedral. On the other hand, encapsulated Pt particles show 4−5 nm in size. This suggests that in the encapsulated method, the particles grow in the pores. This limits their growth to be smaller than the pore size (5.8 nm).

Capping materials such as poly(acrylic acid)[19,25] and poly(N-vinyl-2-pyrrolidone)[27,28] have been typically used as stabilizer in making mono- or bimetallic nanoparticles for protecting aggregation of the metal itself. Specifically, poly(acrylic acid) can be used to control the shapes (tetrahedral, cubic, icosahedral) and sizes of Pt nanoparticles by changing the ratio of the concentration of the capping material to that of the Pt cations in aqueous solution.[19] Though the capping material has advantages such as described above, from a viewpoint of its application to catalysis, it is expected not to have a positive effect due to its partially covering active site of nanosized metal particle. Nevertheless many works have done various hydrogenation over nanometal particles containing polymer.[27−29]

Our Pt/Al_2O_3, prepared using poly(acrylic acid) is characterized by FT-IR to investigate the influence of the polymer on the catalytic activity (shown in Figure 2). Poly(acrylic acid) (Figure 2a) has strong absorption bands at 1570 and 1406 cm^{-1} assigned to the asymmetric and symmetric stretching of the CO_2^- moiety, respectively, and at 1456 cm^{-1} due to the CH_3 rocking.[30] Characteristic bands of Al_2O_3 are observed at 1643 and 1400 cm^{-1}, which are clearly resolved from the polymer bands. Surprisingly, no polymer bands in our as-synthesized Pt/Al_2O_3 are detected. Since only Al_2O_3 characteristic bands are observed in the spectrum shown in Figure 2d. This does not look like the FT-IR spectrum of a mixture of the polymer and the Al_2O_3 shown in Figure 2c. It looks more like that of Pt/Al_2O_3 prepared in the absence of the polymer (shown in Figure 2f). It seems that the length of the polymer (average MW 2100) is too long to be accommodated into the Al_2O_3 channel. From the above results, it can be concluded that the nanoporous Al_2O_3 support fulfills four roles; (1) it gives uniform dispersion and encapsulation of Pt nanoparticles through strong interaction with the Pt salt, (2) it controls the Pt particle size and gives it narrow distribution as determined by Al_2O_3 channel dimensions, (3) it prevents particle aggregation and allows the formation of various shapes such as truncated octahedral, tetrahedral, cubic, and spherical with considerable narrow distribution even in the absence of the capping material, (4) it provides a larger surface area for deposition.

B. Catalytic Hydrogenation of Propene. To evaluate the catalytic activity, hydrogenation of gaseous propene is selected as a test reaction. The propene hydrogenation was carried out in a batch reactor. Prior to the reaction, the catalyst was first preheated at 155 °C for 2 h under an Ar flow and then the reactor was evacuated and held at low pressure and at the same temperature for 10 min. This treatment is carried out in order to remove water and volatile impurities.

The hydrogenation experiments were typically run in the presence of 0.5 g of Pt/Al_2O_3, propene (24 Torr), and hydrogen (165 Torr) at 30−90 °C. The gaseous reaction mixtures were analyzed by mass spectrometry (VG Analytical, 70-SE). The mass spectrum is shown in Figure 3a. The peak at mass number 44.1 is assigned to propane, while that at 42.1 is assigned to propene with a small contribution of propane was calibrated from known standard propene/propane gases mixture. The relative mass peak intensities of propene to propane, observed at any time during the catalyzed reaction, were converted to concentration ratios by use of a predetermined calibration curve (shown in Figure 3b).

The kinetic studies were carried out in following manner. First, a plot of propane concentration vs time is drawn at each temperature studied. The reaction rates as a function of time are determined from the tangent of this plot at different times.

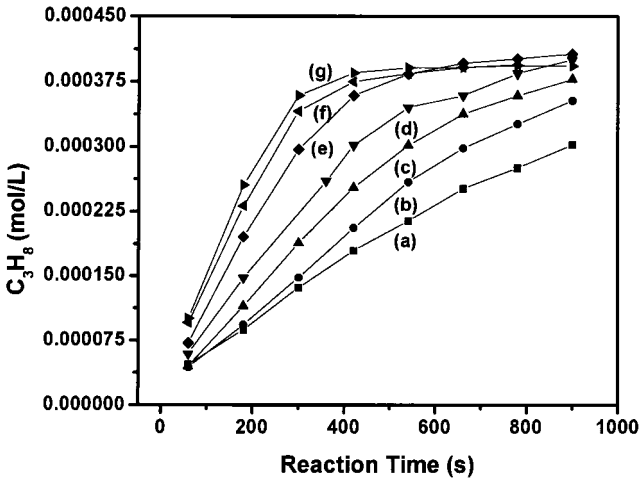

Figure 4. Propane concentration for temperature-dependent propene hydrogenation over Pt/Al_2O_3 catalyst as a function of reaction time: (a) at 30 °C, (b) at 40 °C, (c) at 50 °C, (d) at 60 °C, (e) at 70 °C, (f) at 80 °C, and (g) at 90 °C.

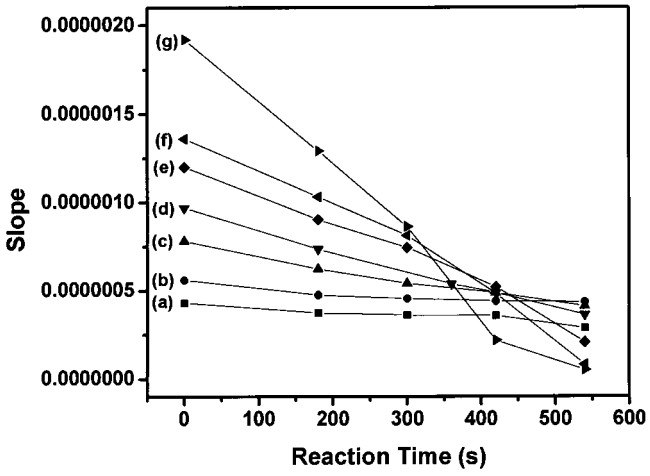

Figure 5. Slope of propane concentration for temperature-dependent propene hydrogenation over Pt/Al_2O_3 catalyst as a function of reaction time: (a) at 30 °C, (b) at 40 °C, (c) at 50 °C, (d) at 60 °C, (e) at 70 °C, (f) at 80 °C, and (g) at 90 °C.

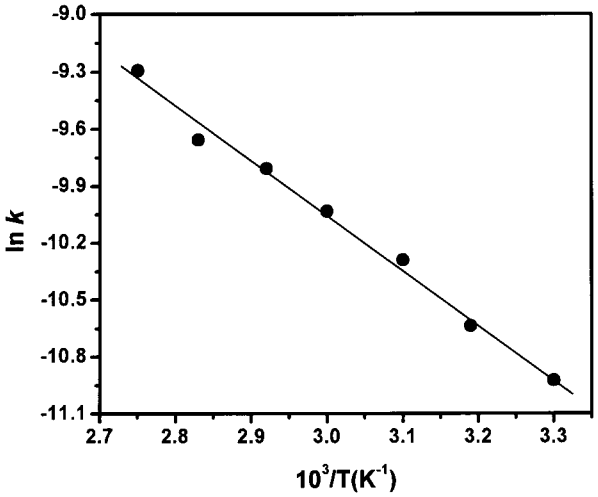

Figure 6. Arrhenius plots of the natural logarithm of rate constant vs $1/T$ for propene hydrogenation over Pt/Al_2O_3 catalyst.

These rates vs time are then plotted to determine the initial rates at different temperatures by extrapolating these lines to zero time. The reaction orders for the propene and hydrogen reaction are obtained from the dependence of the initial rates on the concentration of H_2 and propene at 40 °C. The rate constant (k) at different temperatures is then calculated from the initial reaction rate, the rate equation, the corrected initial H_2, and propene concentrations at each temperature. An Arrhenius plot is then used to determine the value of the activation energy.

The hydrogenation reaction on Pt is quite well studied in terms of specific catalytic activity, kinetic law, and activation energy.[31,32] Under our mild reaction conditions, propane is the only reaction product detected and no deactivation processes are observed during the reaction. These observations are in agreement with the work of Bond et al.[33] who has shown that Pt metal is an effective catalyst to convert propene to propane selectively. The C−C bond cracking/recombination of propene and propane over Pt/Al_2O_3 catalyst under our reaction conditions does not occur. Less than 1% of propane is found to dehydrogenate to produce propene at high temperatures in our reaction. The Pt/Al_2O_3 catalyst gives the propene conversion of 16−39% with 100% selectivity of propane in the reaction times of 9 min at 30−90 °C.

Figure 4 shows a plot of propane concentration vs reaction time in the propene hydrogenation over Pt encapsulated in Al_2O_3 in the temperature range of 30−90 °C. The propane concentration is found to increase almost linearly with time in the range of 30−60 °C but in the 70−90 °C range, the concentration tends to level off slowly and almost reaches steady-state within 9 min. The slope (tangent) of these curves at any time gives the instantaneous rate of the reaction at this time. To determine the initial rate, these tangents (slopes) are plotted as a function of time and extrapolation to zero time at different temperatures gave the initial rate. The results are shown in Figure 5 and the calculated initial rates at different temperatures are given in Table 1.

The reaction is assumed to follow the reaction rate law:

$$\text{initial reaction rate} = k[C_3H_6]^{\alpha}[H_2]^{\beta}$$

where α and β are the order of the reaction with respect to C_3H_6 and H_2, respectively. By determining the initial rates at different reactant concentrations, the α and β are found to be 0.03 and 0.75, respectively. These values are quite similar to those reported by Otero-Schipper et al.[22] for the catalysis over Pd on SiO_2 and TiO_2, suggesting a similar mechanism.

TABLE 1: Initial Rates and Rate Constants of Propene Hydrogenation over Pt/Al_2O_3 at Different Temperatures

T (K)	initial rate ($/10^{-7}$ mol L^{-1} s^{-1})	$[C_3H_6]$ initial ($/10^{-3}$ M)	$[H_2]$ initial ($/10^{-3}$ M)	rate constant ($k/10^{-5}$)
303	4.3	1.27	8.73	1.8
313	5.6	1.23	8.45	2.4
323	7.8	1.19	8.19	3.4
333	9.7	1.16	7.95	4.4
343	12.0	1.12	7.71	5.5
353	13.6	1.09	7.50	6.4
363	19.2	1.06	7.29	9.2

The specific rate constant k at different temperatures is calculated from these initial reaction rates, the reaction order, and the corrected initial H_2 and propene concentrations at the different temperatures shown in Table 1. Figure 6 gives the Arrhenius plots of the natural logarithm of the rate constant vs $1/T$ for the reaction catalyzed by Pt/Al_2O_3. As shown, the normal Arrhenius behavior is observed in the temperature range of 30−90 °C. The activation energy of the reaction is calculated to be 5.7 kcal/mol from the observed slope of the linear part of the Arrhenius plot. The reaction was repeated twice, and the reproducibility is found satisfactory. The variance in the value of the activation energy is found to be less than 5%.

Until now, systematic studies for clear understanding of the effects of Pt nanoparticles size, shape, and capping material (which is usually used in preparation of shaped particle and prevent particle aggregation) on the value of the activation energy in the propene hydrogenation have not been done. Several studies[17,22,34] have simply reported the activation energy for propene hydrogenation catalyzed by Pt supported on SiO_2 and TiO_2. Cocco et al.[17] prepared Pt particles supported on SiO_2 and on different type structured TiO_2 such as anatase and rutile using $Pt(allyl)_2$ precursor through reduction by H_2 in organic solution. The activation energies reported for this reaction are in the range of 12.2−14.9 kcal/mol. TiO_2 support shows lower activation energy and the reaction order for hydrogen than those of SiO_2 and rutile-structured TiO_2 indicates a lower value of 2.3 kcal/mol compared to that for anatase TiO_2 while the reaction orders for hydrogen and propene are almost the same. From the reported results, the activation energy appears to be dependent upon support type and structure. Otero-Schipper et al.[22] reported 10.4 kcal/mol for the activation energy over Pt particle deposited on SiO_2 prepared using H_2PtCl_6 by impregnation. He suggested that the value of the activation energy and turnover number are proportional to the fraction of the metal exposed to reactants for similar hydrocarbon hydrogenation. The lowest value for the activation energy is 7.4 kcal/mol and was obtained by using 1 wt % Pt nanoparticles deposited on external surfaces of SiO_2 with 6.5 nm for the average particle diameter.[34] The reaction orders for hydrogen and propene were 0.5 and 0, respectively. These activation energies, except 7.4 kcal/mol, are about twice as large as our value.

There are three possible reasons for the lower activation energy observed in our system. The effect of support on the activation energy could be one. Another reason is the fact that we are using a batch reactor at relatively high pressure. Mass transport effects could lead to lower activation energy. However, in the reaction of butene hydrogenation using Pt single crystals, it was found that the activation energy is ∼10 kcal/mol when using up to 500 Torr pressure.[35] The third reason for the lower activation energy in our Pt/Al_2O_3 studies could be the higher uniform dispersion of small size (less than 5 nm) of the Pt nanoparticles with shapes formed in the Al_2O_3 channel due to strong interaction between the Pt precursor and the Al_2O_3 support. Small particles with specific shapes have edges, corners, epices, and their surfaces are expected to have many defects. Atoms placed at corners, edges, or at defective sites are expected to be highly catalytically active. In addition, having these particles in close contact with the Al_2O_3 support could add greatly to their high catalytic activity.

Conclusions

Pt nanoparticles were encapsulated in an Al_2O_3 channel by reducing its $(PtCl_4)^{-2}$ with H_2 in the presence of poly(acrylic acid). TEM images showed that the nanoparticles are mainly located inside the Al_2O_3 channel and are highly dispersed. After extraction of the Pt particles from Al_2O_3 channel to observe clear images of the particles size and shapes, various shapes such as truncated octahedral, cubic, tetrahedral, and spherical with narrow distribution of around 5 nm are observed. Comparing to size/shapes of the Pt nanoparticles prepared in K_2PtCl_4 solution with polyacrylate (without Al_2O_3), the particles formed are found to have double the size with mostly truncated octahedral shape. FT-IR results show that the capping material is not present upon formation of Pt nanoparticles in the Al_2O_3 channel. It seems that the polymer length is too long to be accommodated by the Al_2O_3 channel. The nanoporous Al_2O_3 has four important roles in the synthesis of Pt nanoparticles; (1) it gives uniform dispersion and encapsulate them inside the channel due to the strong interaction with the Pt precursor, (2) it controls the Pt sizes distribution as the growth is limited by the narrow Al_2O_3 channels, (3) it protects the particles against aggregation and allows for the formation of various shapes such as truncated octahedral, tetrahedral, cubic, and spherical even in the absence of the capping material, (4) it provides larger surface for deposition.

The Pt/Al_2O_3 catalyst was used for the propene hydrogenation to evaluate its catalytic activity as measured by the value of its activation energy and compare it with other studies that used different supports. The activation energy is found to be 5.7 kcal/mol. This is about one-half the value of the activation energy reported by others. This may be attributed to the fact that the particles are small and have shapes. Small nanoparticles with shapes have many active atoms present on edges, corners, and defective sites. This gives them high catalytic properties. The use of Al_2O_3 support in close interaction with these particles could also account for the observed large activity.

Acknowledgment. Financial support of this work by the National Science Foundation (Grant No. CHE-9727633) is gratefully acknowledged. We are also thank the staff of the mass spectrometry lab and TEM microscopy center for providing the training necessary to carry out this research.

References and Notes

(1) Schmid, G. In *Clusters and Colloids*; VCH: Weinheim, 1994.
(2) Lewis, L. N. *Chem. Rev.* **1993**, *93*, 2693.
(3) Alivisatos, A. P. *Science* **1996**, *271*, 993.
(4) Henglein, A. *Chem. Rev.* **1989**, *89*, 1861.
(5) Colvin, V. L.; Schlamp, M. C.; Alivisatos, A. P. *Nature* **1994**, *370*, 354.
(6) Emory, S. R.; Nie, S. *J. Phys. Chem. B* **1998**, *102*, 493.
(7) Bruchez, M. Jr.; Moronne, M.; Gin, P.; Weiss, S.; Alivisatos, A. P. *Science* **1998**, *281*, 2013.
(8) Chan, W. C. W.; Nie, S. *Science* **1998**, *281*, 2016.
(9) Toshima, N.; Nakata, K.; Kitoh, H. *Inorg. Chim. Acta* **1997**, *265*, 149.
(10) Schmidt, T. J.; Noeske, M.; Gasteiger, H. A.; Behm, R. J. *J. Electrochem. Soc.* **1998**, *145*, 925.
(11) Chen, C.-W.; Serizawa, T.; Akashi, M. *Chem. Mater.* **1999**, *11*, 1381.
(12) Weller, H. *Angew. Chem., Int. Ed. Engl.* **1993**, *32*, 41.
(13) Henglein, A. *J. Phys. Chem.* **1993,** *97*, 5457.
(14) Jackson, S. D.; McLellan, G. D.; Webb, G.; Conyers, L.; Keegan, M. B. T.; Mather, S.; Simpson, S.; Wells, P. B.; Whan, D. A.; Whyman, R. *J. Catal.* **1996**, *162*, 10.
(15) Jacobs, G.; Ghadiali, F.; Pisanu, A.; Borgna, A.; Alvarez, W. E.; Resasco, D. E. *Appl. Catal. A* **1999**, *188*, 79.
(16) Englisch, M.; Jentys, A.; Lercher, J. A. *J. Catal.* **1997**, *166*, 25.
(17) Cocco, G.; Campostrini, R.; Cabras, M. A.; Carturan, G. *J. Mol. Catal.* **1994**, *94*, 299.
(18) Arai, M.; Takada, Y.; Nishiyama, Y. *J. Phys. Chem. B* **1998**, *102*, 1968.
(19) Ahmadi, T. S.; Wang, Z. L.; Green, T. C.; Henglein, A.; El-Sayed, M. A. *Science* **1996**, *272*, 1924.
(20) Toshima, N.; Yonezawa, T.; Kushihashi, K. *J. Chem. Soc., Faraday Trans.* **1993**, *89* (14), 2537.
(21) Somorjai, G. A. In *Introduction to Surface Chemistry and Catalysis*, Wiley: New York, 1994.
(22) Otero-Schipper, P. H.; Wachter, W. A.; Butt, J. B.; Burwell, R. L.; Cohen, J. B. *J. Catal.* **1977**, *50*, 494.
(23) Rampino, L. D.; Nord, F. F. *J. Am. Chem. Soc.* **1942**, *63*, 2745.
(24) Henglein, A.; Ershov, B. G.; Malow, M. *J. Phys. Chem.* **1995**, *99*, 14129.
(25) Li, Y.; Petroski, J.; El-Sayed, M. A. *J. Phys. Chem.* **2000**, *104*, 10956.
(26) Tauster, S. J. *Acc. Chem. Res.* **1987**, *20*, 389.

(27) Liu, M.; Yu, W.; Liu, H.; Zheng, J. *J. Colloids Int. Sci*. **1999**, *214*, 231.
(28) Shiraishi, Y.; Nakayama, M.; Takagi, E.; Tominaga, T.; Toshima, N. *Inorg. Chim. Acta* **2000**, *300*, 964.
(29) Lu, P.; Toshima, N. *Bull. Chem. Soc. Jpn.* **2000**, *73*, 751.
(30) Zinola, C. F.; Gomis-Bas, C.; Estiu, G. L.; Castro, E. A.; Arvia, A. J. *Langmuir* **1998**, *14*, 3091.
(31) Segal, E.; Madon, R. J.; Boudard, M. *J. Catal*. **1978**, *52*, 45.
(32) Zaera, F.; Somorjai, G. A. *J. Am. Chem. Soc*. **1984**, *106*, 228.
(33) Bond, G. C. In *Catalysis by Metals*; Academic Press: New York, 1962; Chapter 11.
(34) Campostrini, R.; Carturan, G.; Baraka, R. M. *J. Mol. Catal*. **1993**, *78*, 169.
(35) Yoon, C.; Yang, M. X.; Somorjai, G. A. *J. Catal.* **1998**, *176*, 35.